5-1-2004

Polybutadiene modified clay and its nanocomposites

Shengpei Su
Marquette University

David D. Jiang
Marquette University

Charles A. Wilkie
Marquette University, charles.wilkie@marquette.edu

Accepted version. *Polymer Degradation and Stability*, Vol. 84, No. 2 (May 2004): 279-288. DOI.

Polymer Degradation and Stability, Vol. 84, No. 2 (May 2004): 279-288. DOI.

Polybutadiene-modified Clay and Its Nanocomposites

Shengpei Su
Department of Chemistry, Marquette University, Milwaukee, WI
David D. Jiang
Department of Chemistry, Marquette University, Milwaukee, WI
Charles A. Wilkie
Department of Chemistry, Marquette University, Milwaukee, WI

Abstract

A butadiene-modified clay was prepared by ionic exchange between sodium montmorillonite and a butadiene surfactant; the butadiene surfactant was obtained from the reaction of vinylbenzyl chloride grafted polybutadiene with a tertiary amine. Nanocomposites of polystyrene, high impact polystyrene, acrylonitrile–butadiene–styrene terpolymer, poly(methyl methacrylate), polypropylene and polyethylene were prepared by melt blending this modified clay with the virgin polymers. The nanocomposites were characterized by X-ray diffraction, transmission electron microscopy, thermogravimetric analysis, cone calorimetry and the evaluation of mechanical properties. A morphological study of PBD-modified clay–polymer nanocomposites shows that all the composites are immiscible micro-composites. The consistency of the result from XRD and TEM with that of cone calorimetry indicates that the cone calorimeter must also be considered as another method to examine the bulk sample and infer if good dispersion of the clay in the polymer has been achieved. The

mechanical properties of the nanocomposites prepared from different methods show that the mechanical properties are, in general, predictable based on the type of dispersion.

Keywords

Nanocomposites, Butadiene, Cone calorimetry, HIPS, ABS, Polypropylene, Polyethylene

1. Introduction

Clay–polymer nanocomposites have been studied extensively for several years; the discovery by the Toyota group that a composite of polyamide-6 with montmorillonite showed significant improvement in many properties, including mechanical properties and heat distortion temperature, may be marked as the beginning of this era [1], [2]. The preparation of nanocomposites may be accomplished by either a polymerization process or blending. In order to produce a nanocomposite with improved properties, the stacked clay layers should be separated into monolayers and show good compatibility with the polymer matrix [3], [4], [5], [6]. Compatibility is normally achieved by ion exchange of the sodium cation with an organophilic 'onium' ion or by complexation of the metal ion in the gallery space with organic compounds [7], [8], [9], [10], [11].

Nanocomposites may be described as either immiscible, if the clay is not well-dispersed and is acting primarily as a filler, or intercalated, if the clay is well-dispersed and the registry between the clay layers is maintained, or exfoliated, also known as delaminated, if this registry is lost.

The typical low molecular weight 'onium' ions that have been used to make the organically modified clays do not normally have high thermal stability; the degradation of the 'onium' ion can begin as low as 200 °C, and in many cases these materials do not give good dispersion in a melt blending operation. This is one reason why only a small number of products are currently in use, after two decades of research, which take advantage of the attributes of nanocomposites and all these use low melting resins, such as polypropylene [12], poly(ethylene-*co*-vinyl acetate) [13] and synthetic rubbers [14].

A polymeric or oligomeric system is potentially a good choice for the organic modification of a clay; these are likely to have a higher thermal stability and, even if degradation does occur, organics may remain in the clay. AMCOL International Corporation has published a series of patents covering the modification of the clay by water-soluble polymers and oligomers. The polymers are polyvinyl pyrrolidone, polyvinyl alcohol and polyvinylimine [15], [16], [17]. The clays were expanded and mixed with thermoplastics or thermoset polymers to form nanocomposites [18]. There are also some reports about the modification of the clay by non-water-soluble polymers like polypropylene [19], [20], [21], [22], polyethylene [23], polystyrene [24], [25], [26], and poly(methyl methacrylate) [25], [26]. The results for almost all these systems show that only immiscible systems can be formed, except for a polystyrene-modified clay in which intercalated and exfoliated nanocomposites have been produced by melt blending in a Brabender mixer [25], [26].

In this paper, we examine new oligomeric surfactants and the clays prepared from these. Herein we report on a butadiene-modified clay, PBD–clay, and the melt blending of this clay with a variety of polymers.

2. Experimental

2.1. Materials

The majority of chemicals used in this study, including vinylbenzyl chloride, polybutadiene (M_n=1800), benzoylperoxide (BPO), *N*,*N*-dimethylbenzylamine, inhibitor removal reagents, polystyrene (PS) (melt flow index 200 °C/5 kg, 7.5 g/10 min, M_w=230,000), high impact polystyrene (HIPS) (melt flow index 200 °C/5 kg, 6 g/10 min), poly(methyl methacrylate) (PMMA) (crystals, M_w=996,000 (GPC), inherent viscosity 1.25), polyethylene (PE) (melt flow index, 190 °C/2.16 kg, 7 g/10 min), and polypropylene (PP) (isotactic, melt flow index, 230 °C/2.16 kg, 35 g/10 min) were acquired from the Aldrich Chemical Co. Acrylonitrile–butadiene–styrene terpolymer (ABS) (Magnum 275, 230 °C/3.8 kg, 2.6 g/10 min) was provided by the Dow Chemical Company, while pristine sodium montmorillonite was provided by Southern Clay Products, Inc.

2.2. Instrumentation

Thermogravimetric analysis (TGA) was performed on a Cahn TG-131 instrument under a flowing nitrogen atmosphere at a scan rate of 10 °C/min from 20 to 600 °C. All TGA results are the average of a minimum of three determinations; temperatures are reproducible to ±3 °C, while the error bars on the fraction of nonvolatile material is ±3%. Cone calorimetry was performed using an Atlas Cone 2 instrument according ASTM E 1354-92 at an incident flux of 35 kW/m^2 or 50 kW/m^2 using a cone shaped heater. Exhaust flow was set at 24 L/s and the spark was continuous until the sample ignited. Cone samples were prepared by compression molding the sample (20–50 g) into square plaques using a heated press. Typical results from cone calorimetry are reproducible to within about ±10%. These uncertainties are based on many runs in which thousands of samples have been combusted [27]. X-ray diffraction was performed on a Rigaku Geiger Flex, 2-circle powder diffractometer; scans were taken from 2ϑ 0.86 to 10, step size 0.1, and scan time per step of 10 s. Bright field transmission electron microscopy (TEM) images of the composites were obtained at 60 kV with a Zeiss 10c electron microscope. The samples were ultramicrotomed with a diamond knife on Riechert-Jung Ultra-Cut E microtome at room temperature or cryogenic temperatures to give ~70 nm thick sections. PP and PE nanocomposites were cut using cryogenic conditions. The sections were transferred from the knife-edge to 600 hexagonal mesh Cu grids. The contrast between the layered silicates and the polymer phase was sufficient for imaging, so no heavy metal staining of sections prior to imaging is required. Mechanical properties were obtained using a SINTECH 10 (Systems Integration Technology, Inc) computerized system for material testing at a crosshead speed of 0.2 inches/min. The samples were prepared both by injection molding, using an Atlas model CS 183MMX mini max molder, and by stamping from a sheet; the reported values are the average of five determinations.

2.3. Synthesis of the grafted polybutadiene

A 40 g portion of polybutadiene (PBD) (M_w=1800) was dissolved in 40 mL of cyclohexane in a 250-mL round flask equipped with a reflux condenser and a stirrer and the mixture was stirred for 5 h under nitrogen. Then a 2 g portion of BPO was added to the solution and the reaction temperature was raised to 70 °C; then 50 mL of hexane solution containing 8 g of inhibitor free vinylbenzyl chloride was slowly added to the flask over an 8 h period and the reaction was kept for an additional 2 h at 70 °C. After cooling the solvent was removed on a rotary evaporator. The residual was washed five times with 500 mL portion of acetone to remove any poly(vinylbenzyl chloride). The product was about 32 g of a colorless liquid. ^{1}H NMR ($CDCl_3$, δ): 8.1–7.9 (br, 1 H), 7.6–7.4 (two br, 1 H), 7.2–6.9 (br, 2 H), 5.8–4.8 (br, 100 H), 4.6–4.4 (br, 3 H), 2.9–2.6 (br, 7 H), 2.2–1.8 (br, 195 H), 1.7–1.6 (br, 8 H), 1.5–1.3 (br, 12 H).

2.4. Synthesis of PBD cationic surfactant

A 200-mL round flask, equipped with a stirrer and condenser, was charged with 30 g of vinylbenzyl chloride grafted PBD, 20 g of *N*,*N*-dimethylbenzylamine and 50 mL of THF. The temperature was raised to 60 °C and kept at this temperature overnight under nitrogen. Half of the solvent was removed on a rotary evaporator and then 100 mL of ethyl acetate was added to the flask to precipitate the ammonium salt. The precipitation was filtered and redissolved and reprecipitated three times. After the solvent was evaporated, 28 g of a soft white soft polymer remained. ^{1}H NMR ($CDCl_3$, δ): 7.8–7.5 (br, 14 H), 5.6–4.8 (br, 100 H), 3.4–2.9 (br, 13 H), 2.9–2.6 (br, 7 H), 2.2–1.8 (br, 195 H), 1.7–1.6 (br, 7 H), 1.5–1.3 (br, 12 H).

2.5. The preparation of PBD-modified clay

A 100 g portion of the ammonium salt was dissolved in 500 mL of THF while 25 g of sodium montmorillonite was dispersed in 1500 mL of distilled water over 48 h. A 2000 mL portion of THF was added to the dispersed clay and vigorously stirred for 2 h, then the ammonium salt was added dropwise to the dispersed clay. A voluminous white precipitate appeared and the slurry was stirred at 40 °C for 24 h. The stirring was stopped and the precipitate was allowed to settle and the supernatant liquid was poured off and a fresh mixture of H_2O and THF (15:85) was added and the slurry was heated, with stirring, for an additional 24 h at 40 °C. Finally the slurry was filtered and the precipitate was recovered and dried in a vacuum oven at 50 °C for 48 h; 269 g of clay was recovered. The sample for TGA was dried overnight at 80 °C in a vacuum oven.

2.6. Preparation of polymer–clay nanocomposites

All the nanocomposites examined in this study were prepared by melt blending in a Brabender Plasticorder at high speed (60 rpm) at 200 °C for PMMA and 190 °C for PS, HIPS, ABS, PP, and PE. The composition of each nanocomposite is calculated from the amount of clay and polymer charged to the Brabender.

3. Results and discussion

In order to permit the formation of an ammonium salt, an adaptation of the graft copolymerization reaction of styrene onto low molecular weigh polybutadiene was used [28]; the reaction is shown in Scheme 1. To remove the poly(vinylbenzyl chloride), which may also be formed, the product was extensively washed with acetone. Chemical shifts in the range δ=8.2–7.2 indicate that some phenyl and benzoyl groups from the decomposition of the BPO were also grafted onto the PBD. The amount of clay used in the ionic exchange process was calculated from the NMR data, based on the ratio of methyl groups to protons on the double bond.

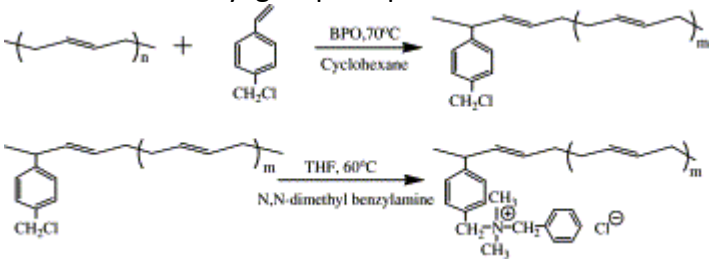

Scheme 1. Preparation of PBD surfactant.

3.1. X-ray diffraction measurements

X-ray diffraction (XRD) is used to determine if any change in the *d*-spacing of the clay has occurred due to nanocomposite formation. The *d*-spacing of the sodium clay is about 1.2 nm and this

increases to about 7.0 nm for the PBD-modified clay. If one observes an XRD peak at a higher *d*-spacing, this is indicative of intercalation. On the other hand, the absence of an XRD peak may mean that either exfoliation has occurred or the clay is disordered. The XRD results are shown in Fig. 1, Fig. 2, Fig. 3, Fig. 4, Fig. 5, Fig. 6 for PS, HIPS, ABS, PMMA, PP and PE, respectively. Some of the data of the PS nanocomposites have been previously reported [29] and will not be included here, but comparisons between the systems will be included. For both PS and HIPS, one can see, at 5% clay, a small peak at slightly lower 2ϑ value. At lower levels of clay and for the other polymers, no peaks are evident. The absence of peaks at low amounts of clay may be simply a concentration effect or it may indicate that some change occurs as the amount of clay is increased. Since peaks are not seen in the majority of cases, XRD cannot be used to identify the type of morphology and transmission electron microscopy must be used to differentiate between exfoliation and disorder.

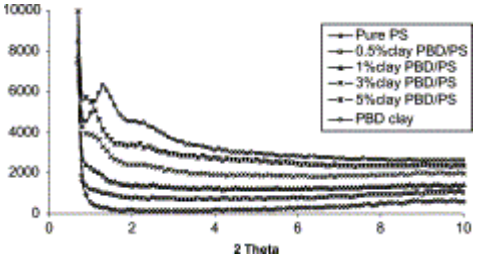

Fig. 1. XRD for PBD clay PS nanocomposites.

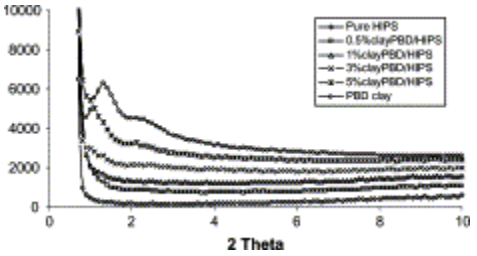

Fig. 2. XRD for PBD clay HIPS nanocomposites.

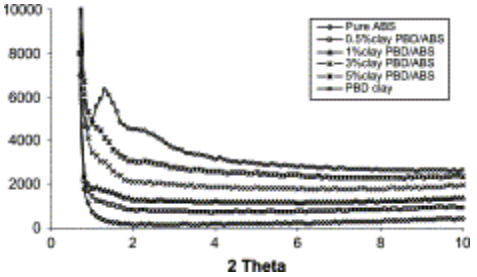

Fig. 3. XRD for PBD clay ABS nanocomposites.

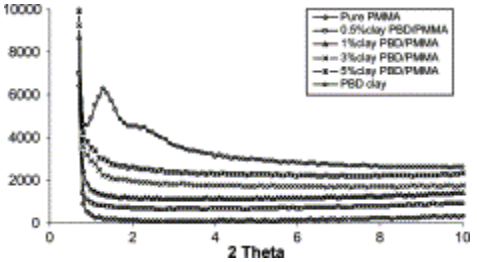

Fig. 4. XRD for PBD clay PMMA nanocomposites.

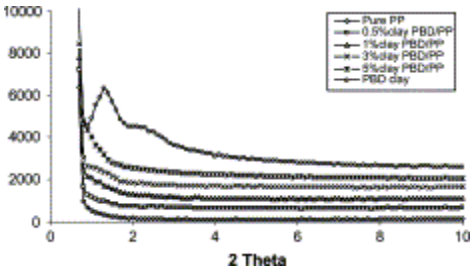

Fig. 5. XRD for PBD clay PP nanocomposites.

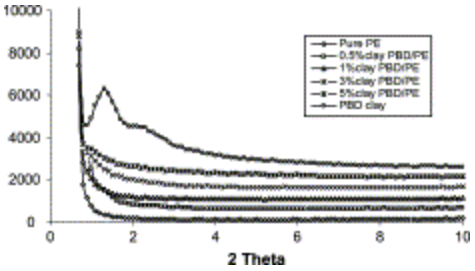

Fig. 6. XRD for PBD clay PE nanocomposites.

3.2. TEM measurement

The TEM image of the PBD clay has been shown previously [29] and it shows a nano-dispersed structure in which one can see what appears to be a droplet-like structure rather than individual clay layers. In the case of polystyrene, the best dispersion was obtained by in situ polymerization and solution blending was more effective than melt blending. Melt blending of PBD clay with polystyrene did not produce a well-dispersed system; a micro-composite was obtained.

Melt blending and melt blending after solution blending were used for the preparation of HIPS nanocomposites. The TEM images of the results from these two processes are shown in Fig. 7, Fig. 8. From the low magnification images, there does not appear to be good dispersion while in the high magnification images, individual intercalated clay layers can be seen. The TEM images of the ABS system (Fig. 9) show very poor dispersion and no individual clay layers can be seen in the high magnification image.

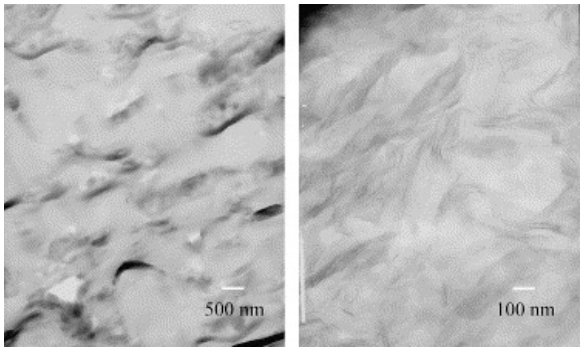

Fig. 7. TEM image at low (left) and at high (right) magnification of PBD clay HIPS nanocomposite by melt blending.

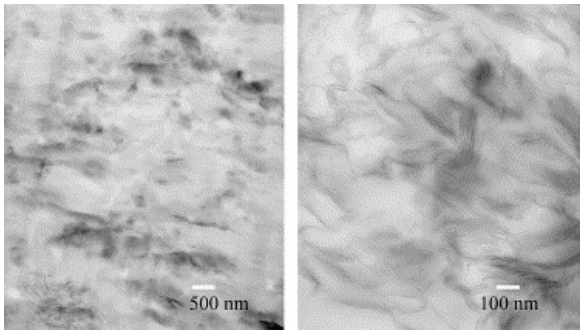

Fig. 8. TEM image at low (left) and at high (right) magnification of PBD clay HIPS nanocomposite by solution, followed by melt blending.

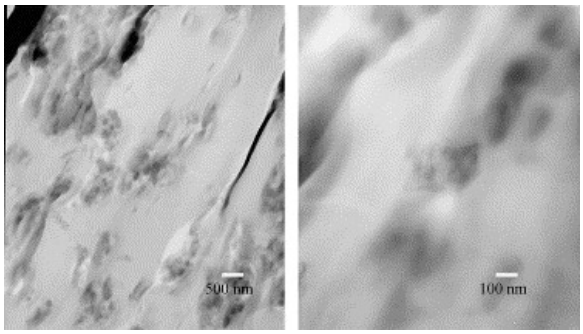

Fig. 9. TEM image at low (left) and at high (right) magnification of PBD clay ABS nanocomposite by melt blending.

PMMA nanocomposites were prepared at higher temperature (about 230 °C), compared to other polymer matrixes and by two different processes, the simple melt blending in which both components are charged to the blender at the same time and a process in which the PMMA is first melted in the blender, followed by the addition of the clay. The TEM image for the first process is shown in Fig. 10while that for the second is shown in Fig. 11. In both cases, tactoids are present in the low magnification image.

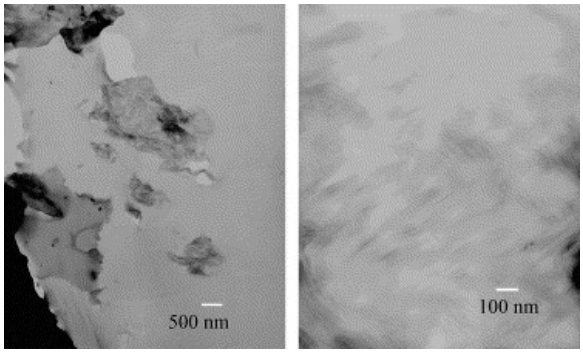

Fig. 10. TEM image at low (left) and at high (right) magnification of PBD clay PMMA nanocomposite by melt blending (PMMA and clay added at the same time).

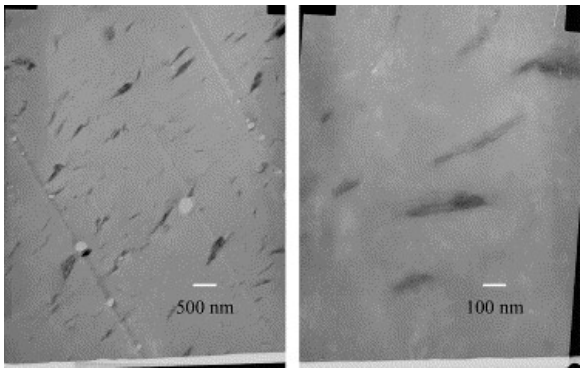

Fig. 11. TEM image at low (left) and at high (right) magnification for PBD clay PMMA nanocomposite by melt blending (PMMA added first, followed by the addition of the clay).

Fig. 12, Fig. 13 show the TEM images for the PBD clay PP nanocomposites by melt and solution blending, respectively. The nano-dispersion is better for the melt blending, but tactoids are still evident and these are more clearly seen in the solution blended system. Similar results are seen for the PE nanocomposites (Fig. 14). One must conclude that none of these systems show good dispersion; all should be categorized as micro-composites, in which the clay is acting mostly as a filler and not as a nano-dimensional phase. In other work [29], it has been shown that better dispersion is obtained by bulk polymerization of styrene in the presence of the PBD clay.

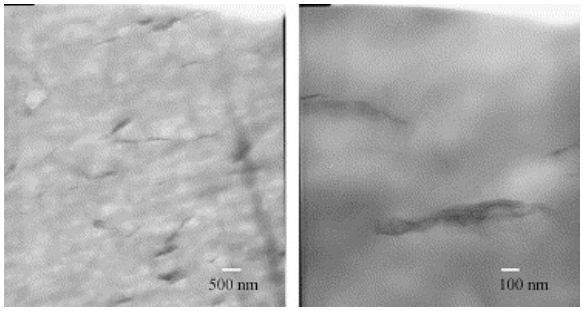

Fig. 12. TEM image at low (left) and at high (right) magnification of PBD clay PP nanocomposite by melt blending.

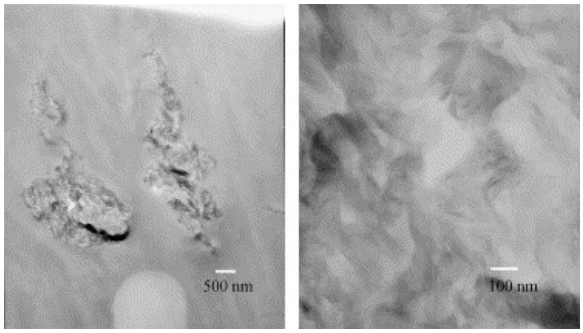

Fig. 13. TEM image at low (left) and at high (right) magnification of PBD clay PP nanocomposite by solution blending.

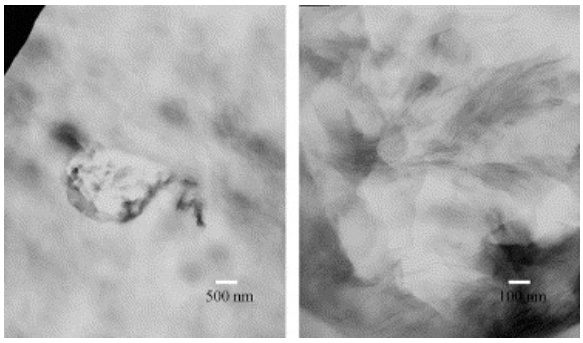

Fig. 14. TEM image at low (left) and at high (right) magnification of PBD clay PE nanocomposite by melt blending.

3.3. TGA characterization of the nanocomposites

The thermal stability of the PBD-modified clay and its nanocomposites were evaluated by TGA. The results are shown in Table 1 and include the temperature at which 10% degradation occurs ($T_{10\%}$), a measure of the onset of degradation; the temperature at which 50% degradation occurs, the mid-point of the degradation process ($T_{50\%}$); and the fraction of material which remains at 600 °C, denoted as char [30]. These results are also presented graphically for each of the polymer systems studied in Fig. 15, Fig. 16, Fig. 17, Fig. 18, Fig. 19, Fig. 20. As the amount of clay increases, $T_{10\%}$ and $T_{50\%}$ increase for all the polymers. PMMA, PS and PP show a greater increase in the onset temperature than is seen in HIPS, ABS or PE. The increase in the 50% point follows the order: PS, PMMA, HIPS > ABS, PP > PE. Based on previous work, one expects to see about a 50 °C increase in the onset temperature for PS with little or no change for the other polymers. These results are unlike those from other organically modified clays, since all polymers appear to show an increase in the onset temperature of the degradation, and further work is necessary to have the opportunity to offer any explanation.

Table 1. TGA analysis of PBD-modified clay–polymer nanocomposites

Materials	**$T_{10\%}$ (°C)**	**$T_{50\%}$ (°C)**	**Char (%)**
Pure PS	390	429	2.0
0.5%PBDclay PSnano	399	435	1.6
1%PBDclay PSnano	411	442	3.3
3%PBDclay PSnano	421	453	5.5
5%PBDclay PSnano	425	459	7.4
Pure HIPS	420	448	0
0.5%PBDclay HIPSnano	420	451	3.0
1%PBDclay HIPSnano	424	453	1.9
3%PBDclay HIPSnano	425	458	5.8
5%PBDclay HIPSnano	431	469	10.7
Pure ABS	407	441	2.5
0.5%PBDclay ABSnano	411	439	2.8
1%PBDclay ABSnano	412	443	4.1
3%PBDclay ABSnano	418	448	5.1
5%PBDclay ABSnano	418	452	6.3
Pure PMMA	287	354	0.5
0.5%PBDclay PMMAnano	283	376	2.3
1%PBDclay PMMAnano	285	379	1.9

3%PBDclay PMMAnano	307	388	3.6
5%PBDclay PMMAnano	324	394	5.9
Pure PP	401	454	0.2
0.5%PBDclay PPnano	418	468	0.4
1%PBDclay PPnano	418	470	0.9
3%PBDclay PPnano	434	479	3.2
5%PBDclay PPnano	435	480	3.8
Pure PE	450	487	0.6
0.5%PBDclay PEnano	457	491	1.6
1%PBDclay PEnano	461	489	3.4
3%PBDclay PEnano	464	495	4.2
5%PBDclay PEnano	465	497	6.3
PBD clay	375	466	29.2

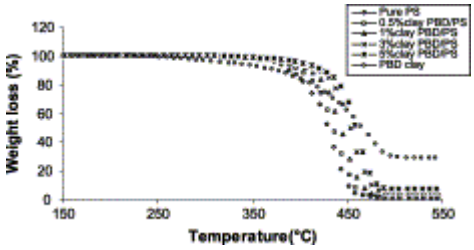

Fig. 15. TGA for PBD clay PS nanocomposites.

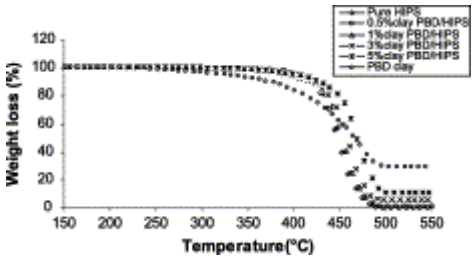

Fig. 16. TGA for PBD-modified clay HIPS nanocomposites.

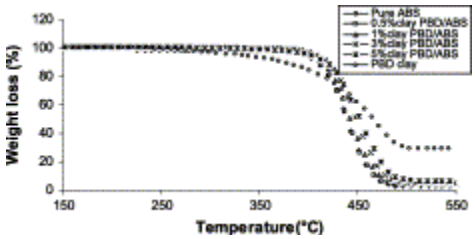

Fig. 17. TGA for PBD clay ABS nanocomposites.

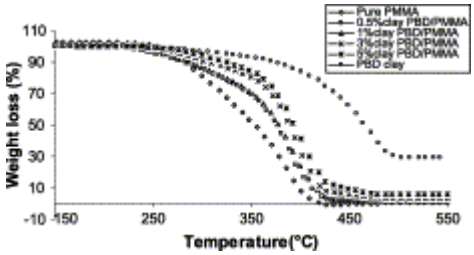

Fig. 18. TGA for PBD clay PMMA nanocomposites.

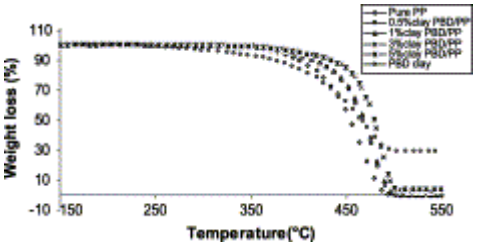

Fig. 19. TGA for PBD-modified clay PP nanocomposites.

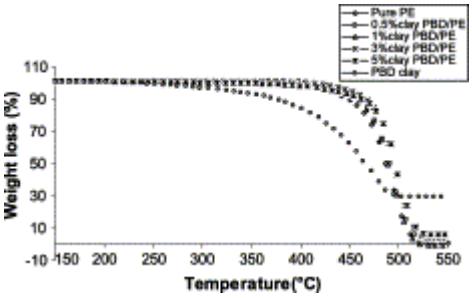

Fig. 20. TGA for PBD clay PE nanocomposites.

3.4. Cone calorimetric characterization of the nanocomposites

The various parameters that may be evaluated using cone calorimetry, including the time to ignition, t_{ign}, the heat release rate curve, especially its peak value, the peak heat release rate, PHRR and the time to PHRR, t_{PHRR}, the mass loss rate, MLR, and the specific extinction area, SEA, a measure of the amount of smoke evolved, are tabulated in Table 2, Table 3, Table 4, Table 5, Table 6, Table 7. It is striking that there is no change in any parameter with less than 5% clay; it must be remembered that the usual spread of values in a cone experiment is ±10%, so any change that is less than 10% is considered to be no change. When 5% clay is present, there is a measurable reduction in PHRR which exceeds the 10% value and this must be considered significant. The conclusion must be that at 5% clay there is some nanocomposite formed and this does serve to give a reduction in PHRR. In previous work, reduction in the PHRR has been seen at as low as 0.1% clay [8]. This was with a clay in which the ammonium counter ion had a molecular weight of about of 500, while this clay is about four times larger. Thus one would expect to see some change at 1% clay, but this is not seen. The time to ignition is either decreased slightly or unchanged for all polymers except PMMA, in which the time to ignition is approximately doubled. The decrease in the PHRR is much less than that expected, based on previous work, for all polymers [25], [26].

Table 2. Cone calorimetric data for PBD-modified clay PS nanocomposites

Composition	**Pure PS**	**0.5%ClayPBD/PS**	**1%ClayPBD/PS**	**3%ClayPBD/PS**	**5%ClayPBD/PS**
Time to ignition (s)	62 ± 5	61 ± 3	61 ± 4	60 ± 1	55 ± 4
PHRR (kW/m^2; % reduction)	1191 ± 35	1196 ± 45 (0)	1183 ± 37 (0)	1109 ± 40 (0)	975 ± 18 (18)
Time to PHRR (s)	122 ± 8	130 ± 4	131 ± 1	124 ± 1	88 ± 19
Time to burn out (s)	238 ± 7	240 ± 3	228 ± 16	242 ± 6	250 ± 6
Average HRR (kW/m^2)	678 ± 29	721 ± 14	727 ± 9	638 ± 37	563 ± 34

Total heat released (MJ/m^2)	94 ± 1	101 ± 1	99 ± 2	94 ± 2	90 ± 1
Average mass loss rate (g/stm^2)	30.3 ± 0.4	29.9 ± 0.7	29.8 ± 0.6	29.3 ± 0.3	27.1 ± 0.7
Average specific extinction area (m^2/kg)	1284 ± 9	1313 ± 9	1332 ± 16	1346 ± 37	1388 ± 15

Table 3. Cone calorimetric data for PBD-modified clay HIPS nanocomposites

Composition	**Pure HIPS**	**0.5%ClayPBD /HIPS**	**1%ClayPBD /HIPS**	**3%ClayPBD /HIPS**	**5%ClayPBD /HIPS**
Time to ignition (s)	70 ± 3	68 ± 2	60 ± 1	56 ± 1	37 ± 4
PHRR (kW/m^2; % reduction)	1183 ± 31	1207 ± 23 (0)	1246 ± 21 (0)	1204 ± 48 (0)	1090 ± 46 (8)
Time to PHRR (s)	118 ± 11	113 ± 1	116 ± 6	83 ± 8	79 ± 3
Time to burn out (s)	211 ± 8	202 ± 6	209 ± 5	224 ± 3	238 ± 4
Average HRR (kW/m^2)	778 ± 16	832 ± 3	834 ± 2	647 ± 6	618 ± 6
Total heat released (MJ/m^2)	103 ± 1	103 ± 1	103 ± 2	100 ± 2	101 ± 2
Average mass loss rate (g/stm^2)	29.4 ± 0.5	29.6 ± 0.6	29.3 ± 0.1	24.1 ± 1.5	26.2 ± 0.7
Average specific extinction area (m^2/kg)	1375 ± 1	1393 ± 13	1432 ± 12	1502 ± 6	1555 ± 13

Table 4. Cone calorimetric data for PBD-modified clay ABS nanocomposites

Composition	**Pure ABS**	**0.5%ClayPBD/ABS**	**1%ClayPBD /ABS**	**3%ClayPBD /ABS**	**5%ClayPBD /ABS**
Time to ignition (s)	61 ± 6	59 ± 3	59 ± 1	56 ± 3	58 ± 6
PHRR (kW/m^2; % reduction)	1237 ± 8	1258 ± 14 (0)	1257 ± 19 (0)	1192 ± 43 (4)	976 ± 24 (21)
Time to PHRR (s)	118 ± 5	118 ± 1	119 ± 2	105 ± 3	103 ± 6
Time to burn out (s)	217 ± 21	214 ± 9	207 ± 6	219 ± 1	219 ± 9
Average HRR (kW/m^2)	753 ± 41	794 ± 5	753 ± 29	742 ± 10	620 ± 8
Total heat released (MJ/m^2)	102 ± 2	101 ± 1	100 ± 1	99 ± 1	93 ± 1
Average mass loss rate (g/stm^2)	28.1 ± 1.2	28.1 ± 0.2	28.2 ± 0.3	26.6 ± 0.7	23.4 ± 0.3
Average specific extinction area (m^2/kg)	1321 ± 18	1348 ± 7	1360 ± 6	1440 ± 17	1483 ± 4

Table 5. Cone calorimetric data for PBD-modified clay PMMA nanocomposites

Composition	**Pure PMMA**	**0.5%ClayPBD /PMMA**	**1%ClayPBD /PMMA**	**3%ClayPBD /PMMA**	**5%ClayPBD /PMMA**
Time to ignition (s)	23 ± 5	21 ± 1	22 ± 1	33 ± 7	52 ± 4
PHRR (kW/m^2; % reduction)	659 ± 10	663 ± 18 (0)	700 ± 31 (0)	641 ± 44 (3)	629 ± 1 (5)
Time to PHRR (s)	92 ± 5	114 ± 4	108 ± 4	109 ± 8	105 ± 2
Time to burn out (s)	196 ± 12	196 ± 15	187 ± 1	202 ± 10	231 ± 16
Average HRR (kW/m^2)	430 ± 3	434 ± 12	466 ± 28	419 ± 20	422 ± 10
Total heat released (MJ/m^2)	70 ± 3	74 ± 1	75 ± 2	72 ± 2	73 ± 2
Average mass loss rate (g/stm^2)	21.6 ± 0.6	21.4 ± 0.2	22.4 ± 0.8	21.4 ± 0.9	21.7 ± 0.1
Average specific extinction area (m^2/kg)	194 ± 12	230 ± 11	273 ± 14	429 ± 5	527 ± 2

Table 6. Cone calorimetric data for PBD-modified clay PP nanocomposites

Composition	**Pure PP**	**0.5%ClayPBD /PP**	**1%ClayPBD /PP**	**3%ClayPBD /PP**	**5%ClayPBD /PP**
Time to ignition (s)	48 ± 2	50 ± 1	47 ± 2	50 ± 1	46 ± 1
PHRR (kW/m^2; % reduction)	1610 ± 89	1468 ± 216 (9)	1481 ± 136 (8)	1420 ± 227 (11)	1191 ± 137 (26)
Time to PHRR (s)	124 ± 1	129 ± 3	127 ± 3	120 ± 8	109 ± 3
Time to burn out (s)	226 ± 14	229 ± 8	217 ± 4	220 ± 13	214 ± 14
Average HRR (kW/m^2)	787 ± 57	767 ± 71	754 ± 25	752 ± 109	685 ± 54
Total heat released (MJ/m^2)	109 ± 4	108 ± 4	105 ± 1	99 ± 3	97 ± 1
Average mass loss rate (g/stm^2)	22.8 ± 0.8	21.9 ± 1.5	22.6 ± 0.7	22.6 ± 1.7	21.7 ± 1.8
Average specific extinction area (m^2/kg)	638 ± 20	713 ± 25	736 ± 15	832 ± 76	871 ± 10

Table 7. Cone calorimetric data for PBD-modified clay PE nanocomposites

Composition	**Pure PE**	**0.5%ClayPBD /PE**	**1%ClayPBD /PE**	**3%ClayPBD /PE**	**5%ClayPBD /PE**
Time to ignition (s)	73 ± 3	71 ± 2	71 ± 5	67 ± 3	68 ± 3
PHRR (kW/m^2; % reduction)	1777 ± 213	1934 ± 168 (0)	2004 ± 165 (0)	1791 ± 105 (0)	1529 ± 14 (14)
Time to PHRR (s)	144 ± 4	141 ± 5	141 ± 2	134 ± 3	128 ± 4
Time to burn out (s)	235 ± 10	230 ± 6	236 ± 7	228 ± 14	234 ± 10
Average HRR (kW/m^2)	831 ± 74	910 ± 80	897 ± 89	856 ± 57	783 ± 33
Total heat released (MJ/m^2)	111 ± 2	115 ± 4	115 ± 2	108 ± 1	103 ± 1
Average mass loss rate (g/stm^2)	24 ± 1.7	25.5 ± 1.1	25.2 ± 1.3	24.2 ± 0.7	23.2 ± 0.3
Average specific extinction area (m^2/kg)	505 ± 21	522 ± 18	538 ± 27	673 ± 30	762 ± 18

The most reasonable explanation for these observations is that the clay is not well-dispersed throughout the polymer and that it is acting as a filler. This is in accord with the XRD and TEM results and this confirms that cone calorimetry may be used to ascertain if nano-dispersion of clay within the polymer has been achieved. TEM examines only a very small portion of the polymer and one small sample will not necessarily be representative of the whole. A new NMR method has been developed which also examines the bulk sample [31]; cone calorimetry must also be considered as another method to examine the bulk sample and infer if good dispersion has been achieved.

There is, unfortunately, no theory as yet to explain the relationship between the reduction in PHRR and dispersion of the clay in the polymer. Until such a theory is developed, one can only state that if the reduction in PHRR is significantly lower than the best value that has been reported for that polymer nanocomposite, then there must be a substantial immiscible component to the nanocomposite. A theory is required before one can correlate the reduction in PHRR with the immiscible component.

3.5. Evaluation of mechanical properties

The mechanical properties of PBD-modified clay micro-dispersed composites are shown in Table 8. There is no apparent trend to the data. The improvement in mechanical properties that is typically noted for nanocomposite formation [7] is not seen, another indication that the clay is not well-dispersed and that it is functioning primarily as a filler.

Table 8. Mechanical properties of PBD clay–polymer nanocomposites

Nanocomposite	**Elongation (%)**	**Modulus (GPa)**	**Tensile strength (Mpa)**
PS	2.5 ± 0.7	1.222 ± 0.141	32.77 ± 6.31
0.5% PBD clay/PS	2.4 ± 0.5	1.345 ± 0.108	34.88 ± 4.83
1%PBD clay/PS	3.1 ± 0.8	1.532 ± 0.142	39.52 ± 5.25
3%PBDclay/PS	2.7 ± 0.7	1.441 ± 0.145	36.70 ± 3.07
5%PBDclay/PS	2.3 ± 0.4	1.293 ± 0.092	33.57 ± 6.60
3%PBDclay/PS(sol)	7.6 ± 2.6	1.361 ± 0.063	25.57 ± 5.04
3%PBDclay/PS(sol-melt)	15.0 ± 8.2	1.360 ± 0.081	32.0 ± 5.24
3%PBDclay/PS(dis-melt)	3.0 ± 1.2	1.483 ± 0.112	34.28 ± 4.02
HIPS	49.4 ± 17.0	1.1114 ± 0.0487	25.85 ± 6.94
0.5%PBDclay/HIPS	32.3 ± 10.1	1.113 ± 0.061	19.91 ± 3.34
1%PBDclay/HIPS	14.4 ± 3.9	1.181 ± 0.072	22.50 ± 2.51
3%PBDclay/HIPS	17.6 ± 5.4	1.104 ± 0.074	16.99 ± 3.47
5%PBDclay/HIPS	18.6 ± 3.7	1.074 ± 0.049	16.72 ± 2.97
3%PBDclay/HIPS(sol)	9.0 ± 0.7	1.017 ± 0.05	15.71 ± 3.49
3%PBDclay/HIPS(sol-melt)	16.1 ± 8.4	1.052 ± 0.04	19.46 ± 1.80
ABS	44.3 ± 9.1	1.173 ± 0.028	42.2 ± 3.6
0.5%PBDclay/ABS	27.1 ± 5.7	1.109 ± 0.062	35.65 ± 2.91
1%PBDclay/ABS	29.2 ± 1.0	1.015 ± 0.019	31.12 ± 2.67
3%PBDclay/ABS	21.7 ± 1.0	1.038 ± 0.054	26.44 ± 4.14
5%PBDclay/ABS	10.1 ± 3.6	0.962 ± 0.061	21.27 ± 2.58
PMMA	2.5 ± 0.7	1.680 ± 0.295	38.67 ± 6.88
0.5%PBDclay/PMMA	2.3 ± 0.5	1.879 ± 0.137	36.21 ± 6.17
1%PBDclay/PMMA	2.1 ± 0.5	1.580 ± 0.275	30.31 ± 9.07
3%PBDclay/PMMA	2.1 ± 0.5	1.656 ± 0.255	34.48 ± 7.80

5%PBDclay/PMMA	2.1 ± 0.5	1.688 ± 0.207	30.76 ± 8.59
PP	769.6 ± 32.2	0.231 ± 0.015	29.02 ± 1.25
0.5%PBDclay/PP	463.8 ± 196.1	0.223 ± 0.018	26.16 ± 1.83
1%PBDclay/PP	216.7 ± 100.1	0.666 ± 0.117	26.49 ± 1.24
3%PBDclay/PP	13.7 ± 1.3	0.660 ± 0.029	20.52 ± 2.73
5%PBDclay/PP	13.9 ± 2.8	0.662 ± 0.028	20.52 ± 0.82
PE	96.0 ± 8.7	0.098 ± 0.005	10.39 ± 0.77
0.5%PBDclay/PE	80.5 ± 11.6	0.100 ± 0.008	10.16 ± 0.88
1%PBDclay/PE	77.0 ± 13.0	0.097 ± 0.006	9.50 ± 0.38
3%PBDclay/PE	53.7 ± 10.5	0.106 ± 0.009	8.47 ± 0.41
5%PBDclay/PE	49.0 ± 4.5	0.108 ± 0.005	7.57 ± 0.34

4. Conclusions

PBD-modified clays do not show promise for nanocomposite formation. This may be due to the lack of compatibility between the low molecular weight polybutadiene and the polymers with which it has been mixed. This work does confirm that cone calorimetry is a good indicator of nano-dispersion.

Acknowledgements

This work was performed under the sponsorship of the US Department of Commerce, National Institute of Standards and Technology, Grant Number 70NANB6D0119.

References

[1] Y Fukushima, A Okada, M Kawasumi, T Kurauchi, O Kamigaito. *Clay Miner*, 23 (1988), p. 27
[2] A Usuki, Y Kojima, M Kawasumi, A Okada, Y Fukushima, T Kurauchi, *et al.. J Mater Res*, 8 (1993), p. 1179
[3] G.E Padawer, N Beecher. *Polym Eng Sci*, 10 (1970), p. 139
[4] J Lusis, R.T Woodhams, M Xanthos. *Polym Eng Sci*, 13 (1973), p. 139
[5] S Cai, G Ji, J Fang, G Xue. *Angew Macromol Chem*, 179 (1990), p. 77
[6] A Garton, S.W Kim, D.W Wiles. *J Polym Sci Polym Lett Ed*, 20 (1982), p. 273
[7] M Alexandre, P Dubois. *Mater Sci Eng*, R28 (2000), pp. 1-6
[8] J Zhu, A.B Morgan, F.L Lamelas, C.A Wilkie. *Chem Mater*, 13 (2001), pp. 3774-3780
[9] E Ruitz-Hitzky, B Casal. *Nature*, 276 (1978), pp. 596-597
[10] Gilman JW, Kashiwagi TA, Morgan B, Harris Jr RH, Brassell L, Award WH, et al. *Proceedings of Additives 2001*; March 2001.
[11] H Yao, J Zhu, A.B Morgan, C.A Wilkie. *Polym Eng Sci*, 42 (2002), pp. 1808-1814
[12] **2002 GMC safari and Chevrolet Astro vans. Step assist** http://www.nanoclay.com/news.html
[13] Sud-Chemie/Kabelwerk Eupen, 2000. *Flameproof polymer composition. PCT Application WO 00/68312*; .G Bayer. *Flame retardants 2002, Interscience Communications*, London (2002), pp. 209-216
[14] ***Wilson/InMat Double Core tennis balls*** http://www.inmat.com
[15] Beall GW, Tsipursky S, Sorokin A, Goldman A. US pat 5552469; 1996.
[16] Beall GW, Tsipursky S, Sorokin A, Goldman A. US pat 5760121; 1998.
[17] Beall GW, Tsipursky S, Sorokin A, Goldman A. US pat 5830528; 1998.
[18] Tsipursky S, Beall GW, Vinokour EI. US pat 5849830; 1998.
[19] M Kato, A Usuki, A Okada. *J Appl Polym Sci*, 66 (1997), p. 1781

[20] M Kawasumi, N Hasegawa, M Kato, A Usuki, A Okada. *Macromolecules*, 30 (1997), p. 6333
[21] N Hasegawa, M Kawasumi, M Kato, A Usuki, A Okada. *J Appl Polym Sci*, 78 (2000), p. 1918
[22] E Manias, A Touny, L Wu, K Strawhecker, B Lu, T.C Chung. *Chem Mater*, 13 (2001), p. 3516
[23] N Hasegawa, H Okamoto, M Kawasumi, M Kato, A Tsukigase, A Usuki. *Macromol Mater Eng*, 280 (2000), p. 76
[24] F.L Beyer, N.C Beck Tan, A Dasgupta, M.E Galvin. *Chem Mater*, 14 (2002), p. 2983
[25] S Su, D Jiang, C.A Wilkie. *Polym Degrad Stab*, 83 (2004), p. 321
[26] S Su, D Jiang, C.A Wilkie. *Polym Degrad Stab*, 83 (2004), p. 333
[27] J.W Gilman, T Kashiwagi, M Nyden, J.E.T Brown, C.L Jackson, S Lomakin, *et al.* S Al-Malaika, A Golovoy, C.A Wilkie (Eds.), *Chemistry and technology of polymer additives*, Blackwell Scientific (1999), pp. 249-265
[28] A Gasperowicz, W Laskawski. *J Polym Sci Polym Chem Ed*, 14 (1976), pp. 2875-2886
[29] Su S, Jiang DD, Wilkie CA. *J. Vinyl Add. Tech*., in press.
[30] A.I Balabanovich, W Schnabel, G.F Levchik, S.V Levchik, C.A Wilkie. M Le Bras, G Camino, S Bourbigot, R Delobel (Eds.), *Fire retardancy of polymeric materials, the use of intumescence,* Royal Society of Chemistry, Cambridge (1998), pp. 236-251
[31] S Bourbigot, J.W Gilman, D.L VanderHart, W.H Awad, R.D Davis, A.B Morgan, *et al. J Polym Sci B Polym Phys*, 41 (2003), p. 3188